Influence of Hydroxyl-Terminated Polybutadiene Additives on the Poly(ether sulfone) Ultra-filtration Membranes

D. Rana,[1] T. Matsuura,[1] R. M. Narbaitz,[2] K. C. Khulbe[1]

[1]*Department of Chemical Engineering, Industrial Membrane Research Institute, University of Ottawa, Ottawa, Ontario, Canada K1N 6N5*
[2]*Department of Civil Engineering, Industrial Membrane Research Institute, University of Ottawa, Ottawa, Ontario, Canada K1N 6N5*

Received 12 July 2005; accepted 4 November 2005
DOI 10.1002/app.23723
Published online in Wiley InterScience (www.interscience.wiley.com).

ABSTRACT: Hydroxyl-terminated polybutadiene (HTPB) was blended into a poly(ether sulfone) (PES) casting solution used to prepare ultra-filtration (UF) membranes via the phase inversion technique. The membranes were then characterized by contact angle (CA) measurements and UF experiments. The CA was increased with the addition of HTPB in the PES membrane and also by lowering the gelation bath temperature. It was observed that the CA was lower for membranes prepared with *N*-methyl-2-pyrrolidinone (NMP) as the solvent than those using *N*,*N*-dimethylacetamide (DMAc) as solvent. The flux values were higher for membranes made using a 4°C gelation bath when compared with the ambient temperature ((25 ± 1)°C) irrespective of the cast solvents, NMP or DMAc. The flux values were much higher and the solute separations were lower for the HTPB-based PES membranes than for the pure PES membrane, when the membranes were cast with DMAc as a solvent. On the other hand, both flux and separation values were much lower for the HTPB-based PES membranes than for the pure PES membrane, when the membranes were cast using NMP. Atomic force microscopy and scanning electron microscopy were used for morphological characterization and the correlation of topography/photography with the performance data was also examined. © 2006 Wiley Periodicals, Inc. J Appl Polym Sci 101: 2292–2303, 2006

Key words: hydroxyl terminated polybutadiene; poly(ether sulfone); contact angle; ultra-filtration; atomic force microscopy; scanning electron microscopy

INTRODUCTION

It is well accepted that from the thermodynamic point of view, the miscibility of polymer blends, i.e. a single phase on the molecular scale, is unusual.[1] If a solution with a blended polymers is equilibrated in the air, the polymer with the lowest surface energy (hydrophobic) will migrate and concentrate at the air interface, as a consequence, reducing the interfacial energy. The preferential adsorption of a lower surface tension component at the surface has been observed for miscible polymer blend systems. Steiner et al.[2] observed in a polyolefin blend system that there was a tendency for the more highly branched component to segregate at the surface when compared with the less branched component, as the former one had a lower surface tension than the later component. Although blending is the classical technique for the membrane surface modification, recently, much attention has been paid in this laboratory to hydrophobic surface modifying macromolecule (BSMM) blending.[3–7] BSMMs are tailor-made to produce surface modification of the membrane, and this approach has been applied for medical, pharmaceutical, food applications as well as industrial chemical processes. Suk et al.[3] studied the surface migration kinetics of BSMM blended membrane. BSMMs migrate to the membrane top surface during the solvent evaporation period as observed by contact angle (CA) and X-ray photoelectron spectroscopy (XPS) measurements. The CA, and the surface fluorine content, as measured by XPS, increased as the solvent evaporation period increased. Zhang et al.[6] noticed that the permeate flux reduction (FR) of the BSMM blended poly(ether sulfone) (PES) flat sheet membrane was much less than for PES membranes without BSMM blending when fouling experiments were conducted with humic acid (HA) solutions. It was observed that the mass of HA deposited on the membrane decreased as the hydrophobicity increased and also as the mean pore size decreased. Recently, tailor-made hydrophilic surface modifying macromolecule (LSMM) was developed and LSMM blended PES

Correspondence to: T Matsuura (matsuura@eng.uottawa.ca).
Contract grant sponsors: Emerging Materials Knowledge program of Materials and Manufacturing Ontario, Natural Science and Engineering Research Council of Canada.

TABLE I
The Characterization Data of the Hydroxyl-Terminated Polybutadiene (HTPB) Additives

Additive code	Manufacturer code	Microstructure (wt %)	Avg. mol. wt. M_n (g mol^{-1})	OH value (meq g^{-1})	Viscosity (Pa s) at 30°C
A	Poly bd R45HTLO	20% vinyl	2800	0.84	5
B	Krasol LBH 2000	65% vinyl	2100	0.91	9
C	Poly bd 605E	20% vinyl	1450	1.74	14.5
D	Krasol LBH-P 3000	65% vinyl	3000	0.64	13

membranes exhibited better fouling resistance when compared with similarly prepared pure PES membranes in the ultra-filtration (UF) performances of the river water.[8]

Considerable attention has been paid to hydroxyl-terminated polybutadiene (HTPB) or modified HTPB (*m*-HTPB) based polyurethane (PU) as a promising material because of its low temperature flexibility, good mechanical performance, and strong resistance to chemical attacks. There are interesting results regarding HTPB or *m*-HTPB-based PU as a membrane material.[9–14] For example, Poussard et al.[9] studied HTPB-based PU membranes incorporating carboxylic groups or ionic species on the soft segment, membrane surface charge increased the membrane hydrophilicity. As a result, fibrinogen adsorption and platelet adhesion were reduced on the PU surface. Gupta et al.[10] studied pervaporation performance using HTPB-based PU, and also poly(urethane-urea) membranes with a 3% phenol–water feed mixture, representative of a very high-strength industrial wastewater. Yang et al.[11,12] studied the wettability and protein adsorption on HTPB-based and *m*-HTPB-based PU membranes. The wettability was enhanced and fibrinogen adsorption on the HTPB-based PU films was decreased.[11] *m*-HTPB-based PU membranes prepared by epoxidation exhibited decreases in albumin and fibrinogen adsorption on the surface.

The surface-modified macromolecule has an amphipathic structure consisting of PU prepolymer end-capped with hydrophobic fluorohydrocarbon (BSMM) or with hydrophilic poly(ethylene glycol) (PEG) (LSMM). Blending BSMMs or LSMMs into the host PES, the surface of the PES membrane becomes more hydro-phobic/-philic. Similarly, HTPB has an amphipathic structure consisting of the central polybutadiene (PB) structure (hydrophobic) terminated by hydroxyl end groups (hydrophilic). Thus, structural similarity convinced us to test HTPB as another series of surface-modified macromolecules, provided that HTPB is miscible with the host PES. At this moment, we are not able to predict whether the surface of the PES membrane becomes more hydrophilic or more hydrophobic, since both PB and hydroxyl end groups may have their effect on the surface properties. Another reason that encouraged us to study the effect of HTPB blending is that no work has been carried out on liquid separation in general and UF in particular, and all of the HTPB or *m*-HTPB-based PU membranes were used in gas separation or pervaporation. Moreover, blending of HTPB into the host polymer has not been attempted.

The objective of this study is, therefore, to evaluate HTPB as a surface-modifying additive for UF PES membranes. The surface of HTPB blended PES membranes, as well as pure PES membranes, are investigated by the static CA, UF, atomic force microscopy (AFM), and scanning electron microscopy (SEM) techniques. The membrane performance is then correlated to the surface properties.

EXPERIMENTAL

Materials

Poly(ether sulfone) (PES; Victrex 4100P) was obtained from Imperial Chemical Industries (ICI), Advanced Materials, Billingham, Cleveland, England. PES was used in this study without further purification but was dried at 80°C for 48 h before used. The molecular weight of PES was 1×10^5 Da. The average molecular weight data was obtained by gel permeation chromatography measurement using polystyrene as a calibration standard. PEG of weight average molecular weight (M_w) 4 kDa was purchased from BDH Inc., Toronto, ON, Canada; PEG 10 kDa from Sigma Chemical Company, St. Louis, MO; and PEG 35 kDa from Fluka Chemie AG, Buchs, Switzerland. The poly(ethylene oxide) (PEO) of viscosity average molecular weight (M_v) 100 and 200 kDa were purchased from Aldrich Chemicals Co, Milwaukee, WI. *N*-Methyl-2-pyrrolidinone (NMP; anhydrous 99.5%) and *N*,*N*-dimethylacetamide (DMAc; 99+%) used as solvents were obtained from Aldrich Chemicals Co. The HTPB additives were kindly supplied by the Sartomer Company, Inc., Oaklands Corporate Center, Exton, PA. The code of all the HTPB additives used in this study is listed in the Table I. The chemical structure of the HTPB additives is presented in the Figure 1.

Preparation of the membranes

PES was used as the base polymer, HTPB was used as an additive, and NMP and DMAc were used as sol-

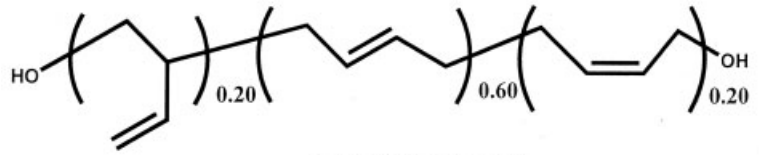

Poly bd R45HTLO (A)

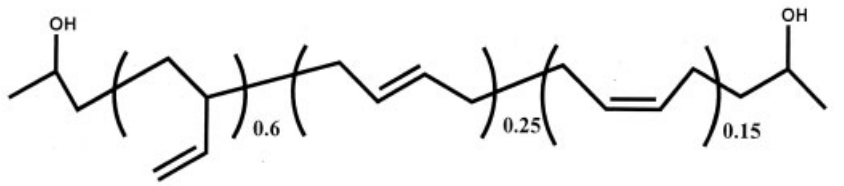

Krasol LBH 2000 (B)

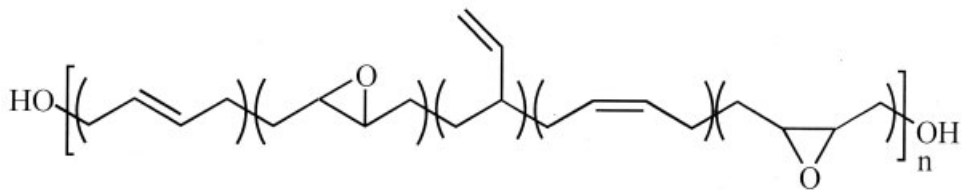

Poly bd 605E (C)

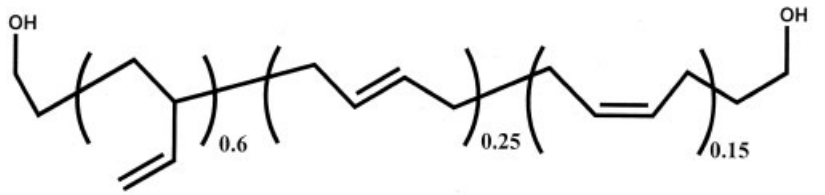

Krasol LBH-P 3000 (D)

Figure 1 The chemical structure of all the used HTPB materials.

vents. The gelation media was water at ambient temperature ((25 ± 1)°C) or at 4°C. The code given to a membrane depends upon the composition of the casting solution and also the temperature of the gelation bath. For example, PES-NMP, PES-NMP-4, and PES-A-NMP represent the membranes made by pure PES in NMP solvent with a gelation media at room temperature, pure PES in NMP solvent and 4°C gelation temperature, and PES with additive-A (i.e., Poly bd R45HTLO) in NMP solvent at room temperature, respectively. The codes of the membranes are shown in Table II. For additives A and B, both NMP and DMAc were used as solvents but for additives C and D, only NMP was used. Visual observation during preliminary tests indicated that the solutions were transparent when 0.5, 1.5, and 3 wt % of HTPB additives were dissolved in NMP solvent, except for 3.0 wt % of HTPB of additive-B in NMP solvent, where the mixture became slightly cloudy. This indicates that micelles could be formed at the high HTPB (additive-B) additive concentration in NMP solvent, which is a common observation for many polymeric surfactants.[15]

The phase inversion technique was used to prepare membranes.[16] The polymeric solution was cast on a glass plate with a casting rod. The thickness of the as-cast film was maintained at 0.2 mm. Then, the solution film together with the glass plate was immersed into a gelation bath containing distilled water at ambient temperature or at 4°C. The membrane peeled off the glass plate spontaneously. The membrane was kept in the gelation bath at least for 24 h before it was used for UF experiments. Prior to the CA measurements, the membranes were blotted dry using a piece of tissue paper and then air dried at room temperature overnight.

When 0.5 wt % of the HTPB additives were blended into the 20 wt % PES solutions, with either NMP or

TABLE II
Composition of the Cast Membranes

Membrane	Base material (wt %)	HTPB additive (wt %)	Solvent (wt %)	Gelation bath temp (°C)
PES-NMP	20% PES		80% NMP	25
PES-NMP-4	20% PES		80% NMP	4
PES-DMAc	20% PES		80% DMAc	25
PES-DMAc-4	20% PES		80% DMAc	4
PES-A-NMP	20% PES	0.5% R45HTLO (A)	79.5% NMP	25
PES-A-DMAc	20% PES	0.5% R45HTLO (A)	79.5% DMAc	25
PES-B-NMP	20% PES	0.5% LBH 2000 (B)	79.5% NMP	25
PES-B-DMAc	20% PES	0.5% LBH 2000 (B)	79.5% DMAc	25
PES-C-NMP	20% PES	0.5% 605E (C)	79.5% NMP	25
PES-D-NMP	20% PES	0.5% LBH-P 3000 (D)	79.5% NMP	25

DMAc as solvent, the membrane looked transparent. However, when the concentration of HTPB additives was increased to 1.5 wt %, the membrane became opaque or phase separated. Therefore, the HTPB concentration was limited to 0.5 wt % in the casting solutions. The compositions of the casting solutions are given in Table II. The PES membranes without HTPB blending and 0.5 wt % HTPB-based PES membranes were characterized by CA, UF, and SEM techniques.

Contact angle measurements

The CA of the membrane surface was measured using a 14° horizontal beam comparator goniometer (model 20–4200, Scherr Tumico, St. James, MN). Sample coupons were prepared by cutting pieces at random locations within the membrane sheets. The samples were placed on glass plates (top membrane surface side up) and fixed with tape. Then, a drop of distilled water (5 μL) was placed on the surface using a microsyringe (Hamilton Company, Reno, NV). The position of the moving bed was adjusted so that the water drop fitted the scale when projected on the screen. The CA was measured at five different locations on each membrane sample at ambient temperature.

Ultra-filtration experiments

The UF experiments were conducted at ambient temperature ((25 $\pm$ 1)°C) using a laboratory-scale system consisting of a reservoir, a pump, a pressure regulator, and six small UF cells connected in series. The cross-flow cells house flat sheet membrane coupons with an effective area of about 13.2 cm^2. The feed flow rate was 2.2 L min^{-1} and the flow characteristics adjacent to the membrane are turbulent. Both the final retentate and all permeates are re-circulated to the reservoir to maintain a uniform feed concentration. The details of the design of the cell and description of the apparatus of UF experiments are given elsewhere.[17,18] All the experiments were conducted at room temperature using an operating pressure of 50 psig. Each membrane was precompressed by filtering pure water at 80 psig for 1 h and then for 4–5 h at 50 psig. Pure water permeation (PWP) rates were measured at 50 psig after the pressurization. This was followed by pore characterization, which used aqueous solutions of various molecular weights of PEGs and PEOs. The feed concentrations of all the PEG and PEO solutions were 200 ppm. The UF system was thoroughly flushed with distilled water between the runs with PEGs or PEOs solutions of different molecular weights. The concentrations of the feed and the permeate solutions were determined via a total organic carbon (TOC) analyzer (model DC-190, Rosemount Analytical Inc., Dohrmann Division, Santa Clara, CA). Two membrane sheets were cast from each casting solution and two coupons were cut from each sheet and the performance of the four coupons was evaluated. Two permeate samples from each coupon were subjected to TOC analysis. Hence, eight permeate samples were available to each coded membrane. For each sample, solute separation (S) was calculated; it is defined as

$$S = 1 - [(C_p - C_w)/(C_f - C_w)] \quad (1)$$

where C_p is the permeate TOC concentration in ppm, C_f is the feed solution TOC concentration in ppm, and C_w is the pure water TOC concentration in ppm. The average values of the separation data so obtained are presented. The mass transfer coefficient is $>100 \times 10^{-6}$ m s^{-1} at the selected feed flow rate, indicating that concentration polarization can be ignored.[17]

Michaels noticed that the log-normal probability function is an accurate way to describe UF membranes sieving curves.[19] The solute separation versus solute diameter data follows a log-normal correlation.[20] Hydrophilic polymers (PEG and PEO) were used as probe solutes to minimize fouling.[21] In this approach, the effects of the steric and hydrodynamic interaction between solute and pores on the solute separation are ignored.

The Einstein-Stokes (ES) radius of solute is a hypothetical sphere that diffuses with the same speed as

the particle under study. Solute radii were calculated based on their average molecular weights.[20] For PEG:

$$R = 16.73 \times 10^{-10} M^{0.557} \quad (2)$$

and for PEO:

$$R = 10.44 \times 10^{-10} M^{0.587} \quad (3)$$

where R is the ES radius in cm and M is the average molecular weight of PEG or PEO in g mol^{-1}.

The molecular weight cut-off (MWCO) value was calculated from the ES diameter of the solute, which gives 90% separation applying either eq. (2) or (3). The mean pore size (μ_p) and corresponding geometric standard deviation (σ_p) can be determined from the solute transport data and it fits a straight line solute separations versus ES diameters graph when plotted on log-normal probability paper. According to the method, the ES diameter that corresponds to 50% of the solute separation is taken as the μ_p, while the ratio between the ES diameter corresponding to the 84.13 percentile of solute separation and that corresponding to 50% is taken as the σ_p. Possible dependence of the solute separation on the steric and hydrodynamic interaction between the solute and the pores is ignored. From the values of the μ_p and σ_p, the pore size distributions of the membranes can be given as a probability density function. The calculations of pore density (N), i.e. the number of pores per unit area, and surface porosity (S_p), the ratio between the areas of pores to the total membrane surface area, were based on the assumption of laminar flow in the membrane pores and the modified Hagen-Poiseuille equation for a porous membrane:[20]

$$N = 128\eta\delta J / \pi \Delta P \Sigma f_i d_i^4 \quad (4)$$

$$S_p = (100 N \pi / 4) \Sigma f_i d_i^2 \quad (5)$$

where η is the solvent viscosity in N s m^{-2}, δ is the length of the pores in μm (considered equivalent to the thickness of the skin layer), J is the solvent flux in m^3 m^{-2} s for pores with diameter d_i in nm, ΔP is the pressure difference across the pores in kPa, f_i is the fraction of pores with diameter d_i. It should be maintained that the thickness of the skin layer of all the membranes, as prepared under the similar protocol, is assumed to be the same, i.e. 0.2 μm. The skin layer thickness 0.2 μm value was well within range of the UF membranes made by various materials as mentioned by other researchers.[20]

AFM topographies studies

An AFM studies were operated on a tapping mode at the top surface area of the dry membrane at ambient temperature in an air environment using a Nanoscope III AFM equipped with a 1533D scanner (Digital Instruments, Santa Barbara, CA) to obtain the topographical information of the membrane surface. Soft organic material surfaces can be successfully imaged with AFM because of the use of micro-fabricated cantilevers.[22–24] The AFM surface morphology is useful to understand the membrane separation performance.[25–33] In the present study, the membrane surface morphology was expressed in terms of the mean surface roughness (R_a). The R_a is the average value of the surface relative to the center plane, i.e. the plane for which the volumes enclosed by the images above and below this plane are equal, and is calculated as

$$R_a = \frac{1}{L_x L_y} \int_0^{L_x} \int_0^{L_y} |f(x,y)| dx dy \quad (6)$$

where $f(x,y)$ is the surface relative to the center plane, and L_x and L_y are the dimensions of the membrane surface. The R_a depends on the treatment of the captured surface data, for example, plane-fitting, flattering, filtering, etc. Therefore, the R_a obtained from AFM images should be considered as relative roughness values. However, in this present study, the same tip was used for all measurements and all captured surfaces were treated in the same protocol.[29,30] The speed of scanning was 2 Hz, and silicon nitride cantilevers were employed. The surface of the dried membranes was compared in terms of the R_a values. The R_a was evaluated from AFM images on different parts of the same scanned membrane and the mean R_a originating from at least five measurements is reported.

SEM photography studies

The SEM was used to observe the cross-sectional area of dry membranes. A model JSM-6400, Japan Electron Optics Limited (JEOL), Japan, was used to generate the SEM photographs. The membrane samples were fractured cryogenically by immersing in liquid nitrogen and then, they were mounted in chair-shaped sample holders with double-sided tape. The fractured surfaces sputter were coated under vacuum with a thin layer of 60% gold and 40% palladium in a sputter system (Hummer VII, Anatech, Springfield, VA).

RESULTS AND DISCUSSION

Contact angle characteristics

The CAs of the HTPB blended PES membranes are slightly higher when compared with the PES membrane without HTPB blending for both NMP and DMAc solvent as presented in Table III. Irrespective of gelation bath temperature and the presence or absence

TABLE III
Contact Angle and UF Characterization Data of the Studied Membranes

Membrane code	Contact angel ($\theta°$)	MWCO (kDa)	Mean pore size (μ_p; nm)	Geometric std. dev. (σ_p)	Pores density (N; pores μm^{-2})	Surface porosity (S_p; %)
PES-NMP	55.6 ± 1.28	15.42	2.20	2.73	113.41	0.43
PES-NMP-4	64.2 ± 1.44	3.01	0.85	2.59	596.91	0.39
PES-DMAc	62.8 ± 1.27	120.75	5.78	2.89	3.92	0.04
PES-DMAc-4	68.5 ± 1.35	51.37	1.75	5.93	5.91	0.03
PES-A-NMP	64.2 ± 1.16	97.73	4.10	3.30	14.88	0.13
PES-A-DMAc	71.8 ± 1.32	196.00	4.19	4.85	41.21	0.36
PES-B-NMP	65.8 ± 1.46	98.88	4.37	3.32	9.18	0.08
PES-B-DMAc	69.8 ± 1.35	123.39	5.35	3.12	18.07	0.20
PES-C-NMP	68.1 ± 1.15	97.66	4.40	3.28	17.04	0.16
PES-D-NMP	68.4 ± 1.06	111.25	4.77	3.27	18.92	0.19

of HTPB additive, the CA of the membranes cast from NMP solvent is lower when compared with DMAc solvent. The CA of membrane increased as the gelation bath temperature decreased for both NMP and DMAc solvent. The change in the CA was relatively small, particularly when compared with many commercial hydro-phobic/-philic blend membranes that have significantly larger/smaller CA. However, hydro-philicity/-phobicity are not the only factors affecting membrane separation and fouling.[34] The CAs of HTPB blended PES membranes are higher probably because of perturbation of the membrane surface morphology by a high proportion of the hydrophobic PB main chain of HTPB, which partially prevented exposure of low proportion of hydroxyl tails to the surface.

Ultra-filtration performances

The normalized flux and solute separation performance of the UF experiments are shown in Tables IV and V, respectively. As expected, as the molecular weight of PEG or PEO solutes increases, the solute separation also increases. In all the membranes in this study, the standard deviation of performance is smaller for higher separation values, which is also expected.

Figure 2 shows the solute separation versus the solute diameter plot on log-normal probability paper. PES-NMP-4, PES-NMP, and PES-A-NMP membranes were chosen to represent the experimental data. Similar plots were obtained for all other membranes. From Figure 2, the mean pore sizes (μ_p) of the PES-NMP-4, PES-NMP, and PES-A-NMP membranes are about 0.85, 2.20, and 4.10 nm, respectively. Accordingly, one would expect lower separations for the HTPB-A modified PES-NMP membranes. Figure 3(a) shows the probability density function versus pore size for PES-NMP and PES-NMP-4 membranes. The pore size distribution is narrower for PES-NMP-4 membrane when compared with the PES-NMP membrane. Figure 3(b) shows that the probability density function versus pore size for four membranes that contain additives (A, B, C, and D) are very similar. Note that all four membranes were cast under the same conditions (i.e. NMP solvent and room temperature gelation bath).

MWCO, mean pore size, geometric standard deviations, pores density, and surface porosity data are summarized in Table III. From this it is evident that the MWCO decreases by lowering the gelation bath temperature for both solvents (i.e. NMP and DMAc). The HTPB blended membranes have higher MWCO than the pure PES membrane. The mean pore size of

TABLE IV
Normalized Flux ($\times 10^{-2}$ L m^{-2} h^{-1} kPa^{-1}) Data of the Membranes for Pure Water Permeation (PWP) and for Various Solutes Solution

Membrane code	PWP	PEG (4 kDa)	PEG (10 kDa)	PEG (35 kDa)	PEO (100 kDa)	PEO (200 kDa)
PES-NMP	47.19 ± 1.77	37.22 ± 1.27	32.81 ± 0.71	27.47 ± 0.62	23.93 ± 0.35	21.05 ± 0.62
PES-NMP-4	17.45 ± 0.82	16.03 ± 0.65	14.75 ± 0.24	13.96 ± 0.65	11.55 ± 0.24	10.65 ± 0.17
PES-DMAc	7.60 ± 0.31	6.08 ± 0.22	5.32 ± 0.16	3.38 ± 0.15	2.43 ± 0.15	2.20 ± 0.22
PES-DMAc-4	5.32 ± 0.48	3.45 ± 0.38	2.66 ± 0.19	1.95 ± 0.05	1.77 ± 0.09	1.59 ± 0.02
PES-A-NMP	21.29 ± 0.69	19.12 ± 0.51	17.98 ± 0.44	15.95 ± 0.38	11.01 ± 0.30	10.41 ± 0.13
PES-A-DMAc	64.59 ± 2.30	57.86 ± 1.11	48.08 ± 1.66	43.27 ± 0.69	23.30 ± 0.53	26.89 ± 0.53
PES-B-NMP	14.06 ± 0.30	12.92 ± 0.24	12.66 ± 0.22	12.66 ± 0.22	9.30 ± 0.17	8.94 ± 0.04
PES-B-DMAc	33.08 ± 1.67	29.25 ± 0.88	26.58 ± 1.77	25.11 ± 0.51	20.00 ± 0.54	13.68 ± 0.10
PES-C-NMP	26.14 ± 1.08	23.93 ± 0.50	23.04 ± 1.53	19.64 ± 0.67	14.77 ± 0.22	13.35 ± 0.10
PES-D-NMP	31.41 ± 0.82	29.63 ± 0.43	26.63 ± 0.41	26.85 ± 0.20	11.06 ± 0.17	10.18 ± 0.09

TABLE V
The Solute Separation (%) Data of the Membranes

Membrane code	PEG (4 kDa)	PEG (10 kDa)	PEG (35 kDa)	PEO (100 kDa)	PEO (200 kDa)
PES-NMP	63.05 ± 0.28	80.60 ± 0.44	98.65 ± 0.09	98.86 ± 0.18	99.52 ± 0.17
PES-NMP-4	90.74 ± 0.38	97.11 ± 0.92	99.86 ± 0.44	99.92 ± 0.12	99.96 ± 0.05
PES-DMAc	33.75 ± 1.16	45.04 ± 0.68	74.59 ± 1.48	92.02 ± 0.64	94.37 ± 1.03
PES-DMAc-4	56.74 ± 1.09	78.65 ± 0.38	88.45 ± 0.35	96.42 ± 0.79	98.14 ± 0.37
PES-A-NMP	54.62 ± 1.38	59.33 ± 2.43	71.76 ± 4.61	98.51 ± 0.10	98.70 ± 0.66
PES-A-DMAc	47.14 ± 1.36	55.77 ± 2.17	66.59 ± 3.70	86.16 ± 0.42	89.57 ± 0.24
PES-B-NMP	41.61 ± 2.14	58.38 ± 1.70	75.08 ± 2.54	96.88 ± 0.25	97.34 ± 0.22
PES-B-DMAc	37.05 ± 1.27	51.40 ± 1.10	67.90 ± 1.41	93.81 ± 0.93	95.22 ± 0.22
PES-C-NMP	41.10 ± 1.74	59.33 ± 0.97	73.49 ± 2.69	97.56 ± 0.22	97.99 ± 0.66
PES-D-NMP	36.68 ± 1.91	61.12 ± 2.12	69.58 ± 1.67	93.78 ± 0.08	97.03 ± 0.45

the HTPB blended membranes is larger than PES membrane without blending when cast from NMP solvent, whereas the mean pore size is slightly smaller than pure PES membrane when cast from DMAc solvent.

In the absence of HTPB, the normalized flux and separation performance data (Tables IV and V) depend upon the casting solvent as well as gelation bath temperature. The fluxes are higher, whereas solute separation efficiencies are lower for membranes prepared using a gelation bath at ambient temperature ((25 ± 1)°C) when compared with the gelation bath at 4°C irrespective of whether the solvent was NMP or DMAc. This is probably due to the formation of thicker dense layer at 4°C gelation due to the slower solvent–nonsolvent exchange. Both flux and separation data are higher for NMP solvent than DMAc solvent in the PES membrane without HTPB additive. It should be mentioned that membrane cast from NMP solvent has higher porosity when compared with the DMAc cast membrane (Table III). It is also noted that the solvent exchange rate is higher for casting solution with DMAc solvent when compared with NMP solvent. Other researchers had also similar observations on solvent dependency of the membrane performance.[35–38] Kesting[35] demonstrated that the molecular size of the casting solvent is a more important parameter than its strength (solubility parameter)

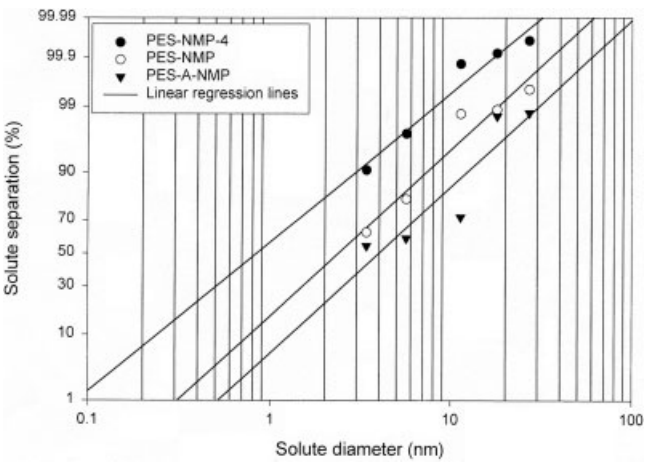

Figure 2 Solute separation versus solute diameter on log-normal plot (The solute diameter of PEG/PEO was calculated according to the average molecular weight).

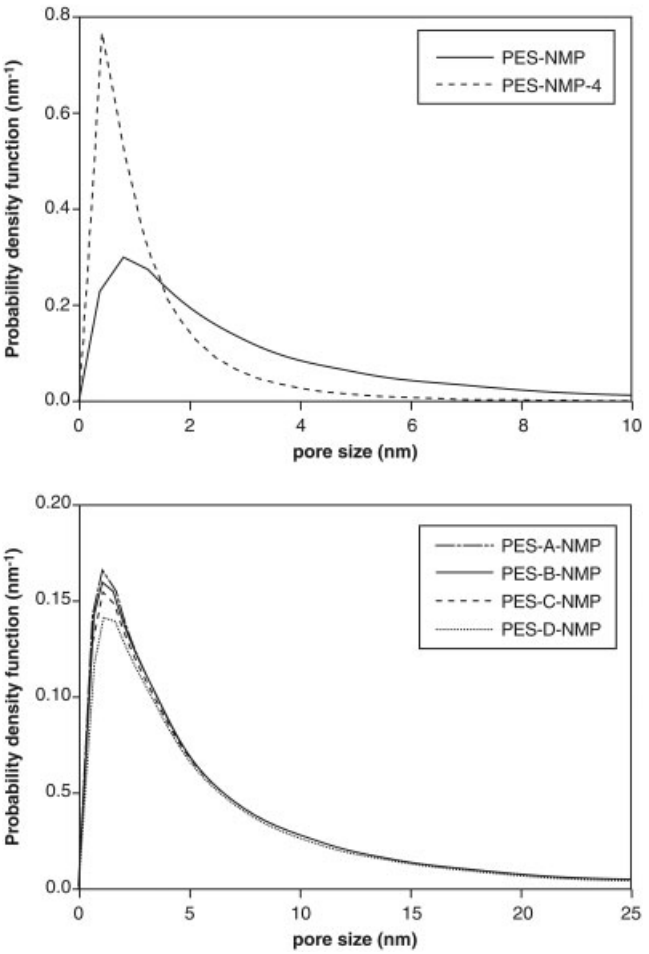

Figure 3 Representative plot of probability density versus pore size as from UF solute transport data: (a) PES-NMP-4 and PES-NMP membranes; (b) PES-A-NMP, PES-B-NMP, PES-C-NMP, and PES-D-NMP membranes.

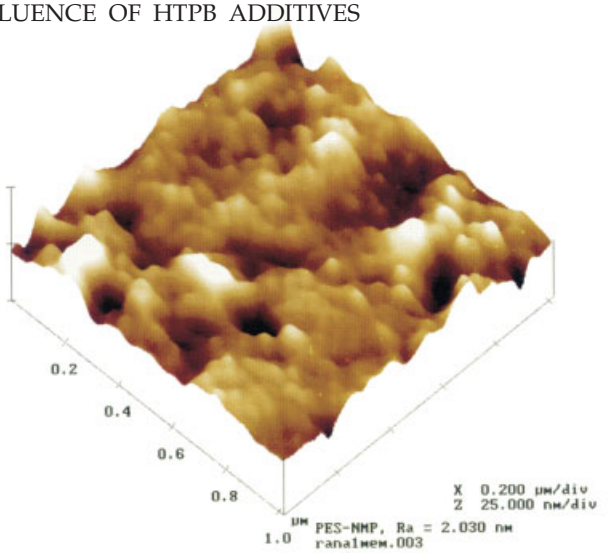

(a) PES-NMP, R_a = 2.030 nm

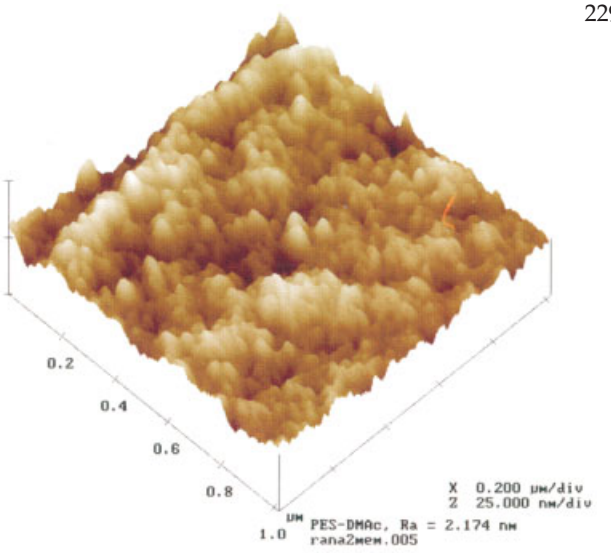

(b) PES-DMAc, R_a = 2.174 nm

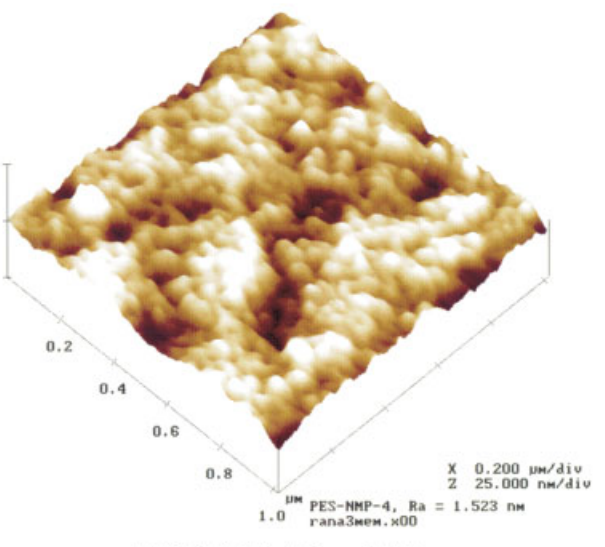

(c) PES-NMP-4, R_a = 1.523 nm

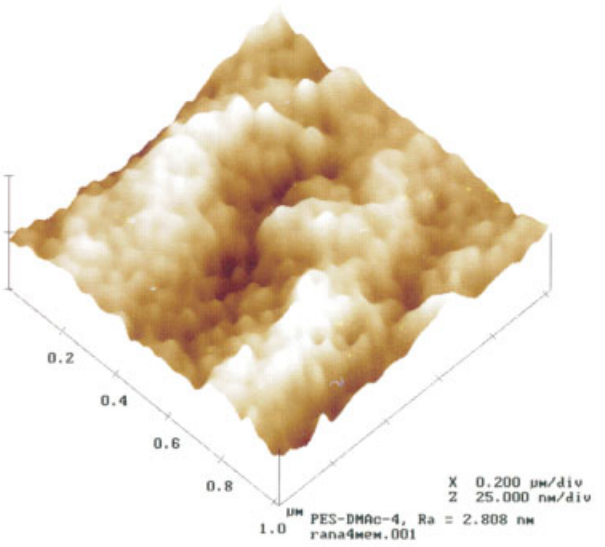

(d) PES-DMAc-4, R_a = 2.808 nm

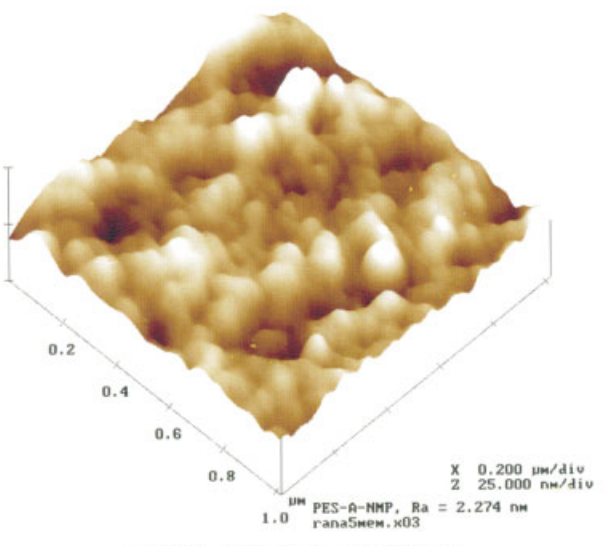

(e) PES-A-NMP, R_a = 2.274 nm

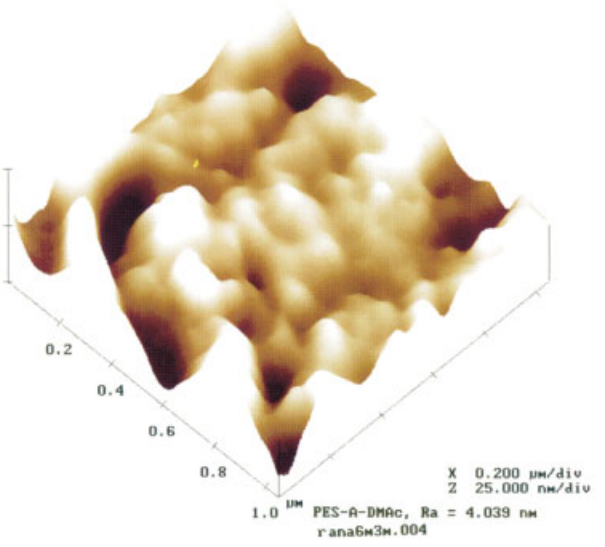

(f) PES-A-DMAc, R_a = 4.039 nm

Figure 4 3D-AFM images at 1 μm scan range of the top surface of the membranes: (a) PES-NMP; (b) PES-DMAc; (c) PES-NMP-4; (d) PES-DMAc-4; (e) PES-A-NMP; (f) PES-A-DMAc[Color figure can be viewed in the online issue, which is available at www.interscience.wiley.com.].

in determining the permeability in the skins of hollow-fiber polysulfone membrane prepared by phase inversion method.

Regarding the effect of HTPB blending, it is difficult to come to any strong conclusions. But, it should be emphasized that a more than eightfold increase of membrane flux was achieved by blending HTPB (additive-A) into PES solution in DMAc solvent as presented in Table IV. As a result, this membrane became the highest flux membrane among all those studied. Judging from the highest hydrophobicity (CA value) and the lowest separation of high molecular weight PEG and PEO, the large water droplets dispersed in the polymer phase led to the largest pore size of this membrane. The high flux of this membrane will also be discussed in view of SEM pictures.

The difference in the solvent for the casting solution can be discussed in the following two aspects. One is the affinity between the solvent and water (nonsolvent). When a cast film is immersed into a gelation media (water), exchange between the solvent and water takes place at the water/polymer solution film interface. When the affinity between solvent and water is higher, more water is drawn into the polymer solution film and the water content in the resulting membrane becomes higher. The affinity between solvent and water can be given by the closeness of solubility parameter of solvent to that of water. Comparing solubility parameters of NMP (11.3 $cal^{1/2}\ cm^{-3/2}$) and DMAc (10.8 $cal^{1/2}\ cm^{-3/2}$), NMP is closer to water (23.4 $cal^{1/2}\ cm^{-3/2}$).[39] Therefore, more water is drawn into the film cast from the solution containing NMP solvent. The other aspect is the density of the solvent. It is known that the solvent of higher density leads to higher water content in the resulting membrane.[16] In this aspect also the density of NMP (1.033 g cm^{-3}) is higher than that of DMAc (0.937 g cm^{-3}) at 20°C.[40] Probably, either solvent/water affinity or density or both may be the reason for the higher water content of the membranes cast from NMP solvent. This is well demonstrated by the SEM pictures shown later. It is also natural to conclude that the membrane of higher water content shows higher permeation rate. The effects of the solvent on HTPB blended membranes are still unknown.

AFM images analysis

The AFM topography of the top membrane surface in 3D images is displayed in Figure 4. The vertical color density shows that the dark regions are the pores (or pore) of the membrane, whereas bright high regions (may be mountains or valleys) are the nodular (or nodule aggregates) structures.[41–43] The NMP solvent created membranes with lower mean surface roughness (R_a) when compared to the DMAc solvent cast PES UF membranes. It is worth noting that for dense membrane of high molecular weight of sulfonated poly(2,6-dimethyl-1,4-phenylene oxide), the R_a value was lower when the membrane were cast from NMP than it was cast from DMAc.[44] The PES-A-DMAc and PES-NMP-4 showed the highest and the lowest R_a value of all the studied membranes, respectively. In the present studied membranes, addition of HTPB additive increases slightly the R_a of PES UF membranes irrespective of the casting solvents.

The relationship between the MWCO and R_a is depicted in Figure 5(a). The membranes tested show a general trend of increasing MWCO with increasing R_a. Several researchers have observed linear relationships between MWCO and R_a.[5,20,45–47] Bessières et al.[46] noticed that the R_a value increased with an increase in MWCO for the sulfonated polysulfone UF membranes. Singh et al.[20] demonstrated that with increasing MWCO, the R_a value increased for PES UF membranes. They explained this relationship in terms of the aggregation of the polymeric nodules that were

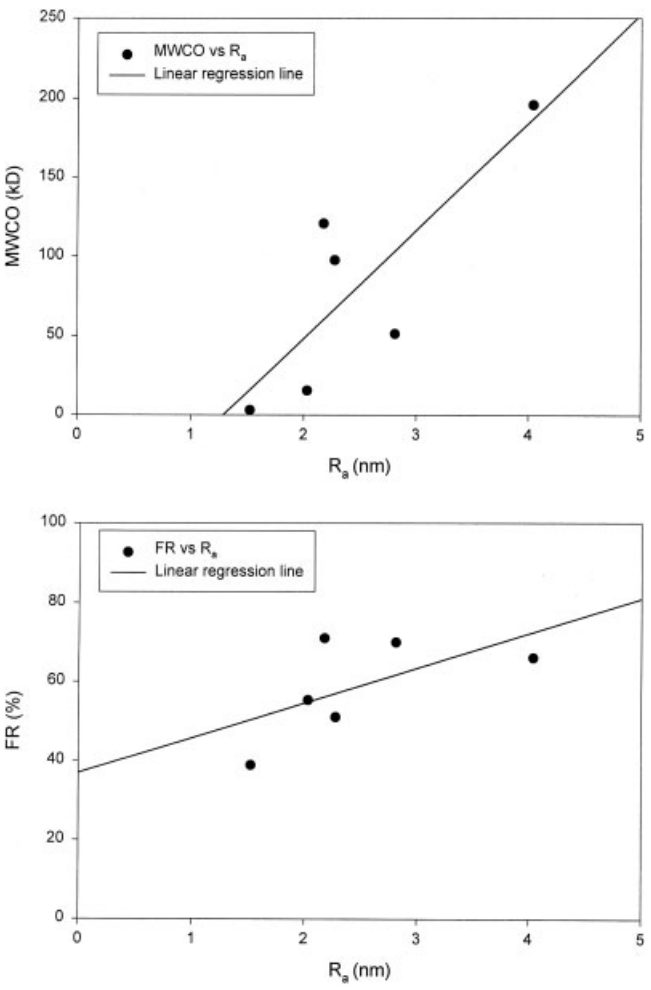

Figure 5 Relationship between AFM top membrane surface roughness with UF performances (pure PES and modified PES membranes): (a) MWCO versus R_a; (b) FR versus R_a.

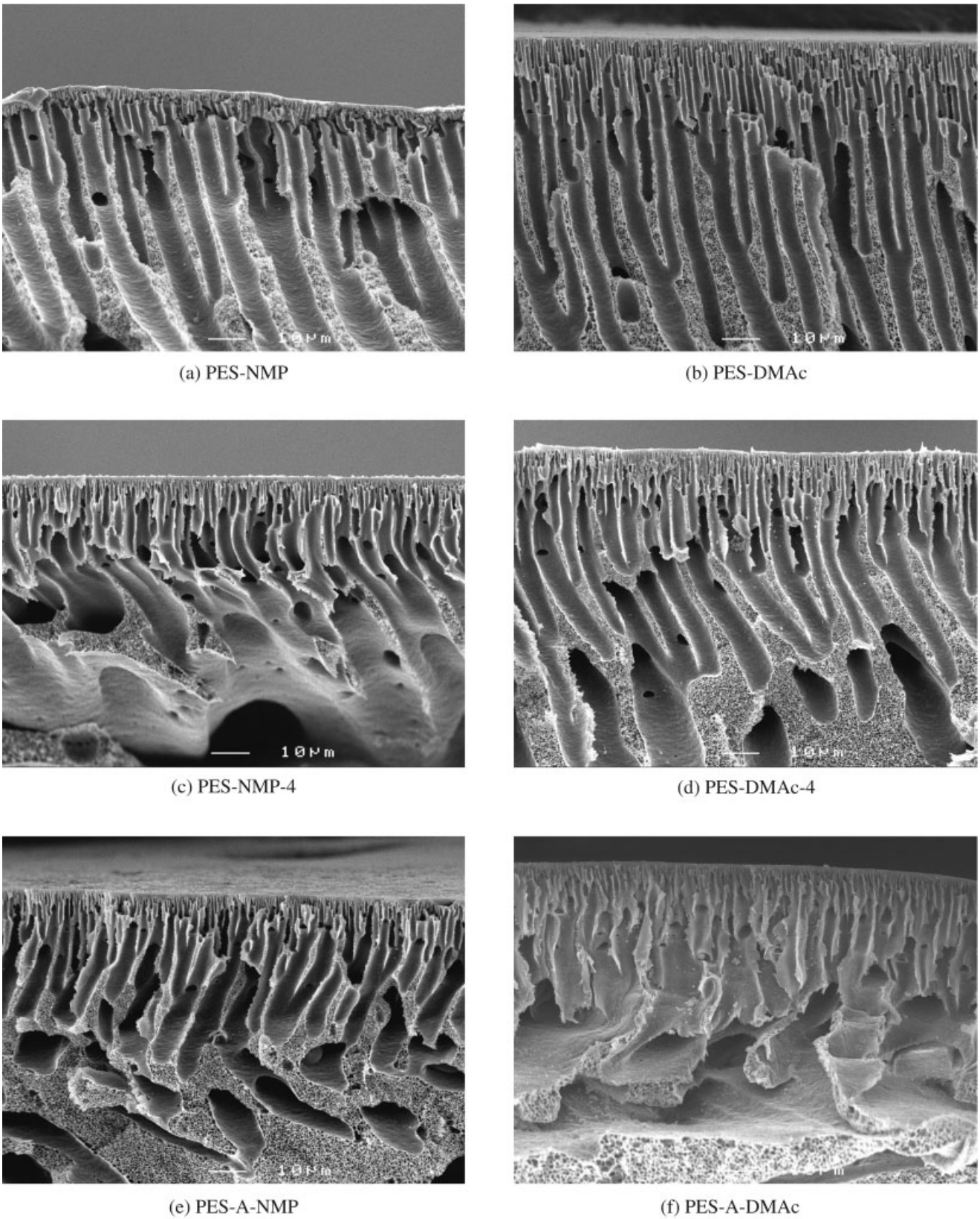

(a) PES-NMP (b) PES-DMAc

(c) PES-NMP-4 (d) PES-DMAc-4

(e) PES-A-NMP (f) PES-A-DMAc

Figure 6 SEM photograph of the cross section surface of the membranes: (a) PES-NMP; (b) PES-DMAc; (c) PES-NMP-4; (d) PES-DMAc-4; (e) PES-A-NMP; (f) PES-A-DMAc.

less tightly packed when the membranes were cast from the solutions having lower concentrations of polymer. Khayet et al.[5] observed that MWCO increased with increasing R_a in their SMM containing poly(ether imide) UF membranes.

The relationship between the FR and R_a is shown in Figure 5(b). The FR is defined as

$$FR\ (\%) = 100\ (1 - PF/PWP) \qquad (7)$$

where PF is the permeate flux when PEO of 200 kDa is used as a solute in the feed solution. The higher the FR value, the more severe the reduction in the flux when a PEO solution is filtered. Most likely, the FR was caused by the high molecular weight macromolecules that partially block the pores. A reasonably good linear relationship is found between FR versus R_a as shown in the Figure 5(c). Other researchers also reported similar observations.[48–50] Elimelech et al.[48] observed higher fouling rate for TFC type polyamide RO membrane when compared with cellulose acetate membrane for their colloidal fouling when the membrane surface was studied by AFM. They claimed that the R_a played an important role in enhancing the attachment rate between colloidal particles and TFC membranes surface. They also demonstrated that the colloidal particles preferentially accumulate in the valleys of rough TFC membrane surfaces causing more severe FR when compared with the smooth cellulose acetate membrane surfaces. Vrijenhoek et al.[49] observed a strong correlation between R_a and flux decline presumably because of colloidal particles fouling on the nano-filtration and RO membranes. Bowen et al.[50] noticed that the clean water FR is greater for higher R_a membranes although similar MWCO value.

SEM micrographs analysis

The SEM micrographs of the cross section of the membranes are presented in the Figure 6. They all possess asymmetric structures with a top skin layer, an intermediate layer of fully finger/sponge-like arrangement, and a bottom layer of fully developed macropores as observed by other researchers.[51–53] The higher flux of the NMP cast membrane when compared with the DMAc cast membrane could be explained in following way. Although both PES-NMP and PES-DMAc have the finger-like shapes, the width of the channels is bigger for membranes prepared with NMP than those prepared with DMAc. Concurrently, the thickness of the support layer is thinner for NMP than for DMAc solvent. So, the resistance of the liquid pass through the NMP solvent is lower than the DMAc solvent.

Interestingly, the SEM picture of PES-A-DMAc membrane, which showed the highest flux, reveals a large void space on the bottom side of the membrane. At the very bottom, a thin sponge-like layer is seen. The presence of this void space may have contributed to the high flux of the membrane. However, the SEM cross-sectional picture earlier cannot predict the membrane flux, since the latter flux is controlled largely by the structure of the top skin layer, which cannot been observed by SEM.

CONCLUSIONS

The following conclusions are drawn from the experimental observations:

1. The CA increases with the addition of HTPB in the PES membranes. Irrespective of gelation bath temperature, the CAs of the membranes cast-using NMP as a solvent are lower when compared with those prepared using DMAc as a solvent. The CA of membrane increases as the gelation bath temperature decreases for both NMP and DMAc solvent.
2. Both fluxes and separation efficiencies are higher for membranes prepared using NMP as a solvent when compared with that for membranes prepared with DMAc. The flux data are higher, whereas solute separations are lower for the gelation bath at ambient temperature when compared with the 4°C irrespective of solvents. On addition of HTPB, the flux data for DMAc solvent increases, whereas for NMP solvent decreases although the separation efficiencies are not much affected.
3. The mean pore size of the HTPB blended membranes is larger than PES membrane as cast from NMP solvent, whereas the mean pore size is smaller for DMAc solvent. HTPB blended membranes have broader pore size distributions when compared with the pure PES membrane irrespective of casting solvent and gelation bath temperature.
4. The MWCO and FR increased with surface roughness as measured by AFM imaging.

The hydroxyl-terminated polybutadiene (HTPB) additives are kindly provided by the Sartomer Company, Inc., Oaklands Corporate Center, Exton, PA. We are also indebted to Dr. Wondeok Lee, Department of Chemical Engineering, University of Ottawa, for the technical assistance of CA and UF measurements.

References

1. Katime, I. A.; Iturbe, C. C. In Polymeric Materials Encyclopedia; Salamone, J. C., Ed.; CRC: Boca Raton, FL, 1996; Vol. 5, p 3097.
2. Steiner, U.; Klein, J.; Eiser, E. Science 1992, 258, 1126.
3. Suk, D. E.; Chowdhury, G.; Matsuura, T.; Narbaitz, R. M.; Santerre, J. P.; Pleizier, G.; Deslandes, Y. Macromolecules 2002, 35, 3017.
4. Khayet, M.; Chowdhury, G.; Matsuura, T. AIChE J 2002, 48, 2833.
5. Khayet, M.; Feng, C. Y.; Matsuura, T. J Membr Sci 2003, 213, 159.

6. Zhang, L.; Chowdhury, G.; Feng, C.; Matsuura, T.; Narbaitz, R. J Appl Polym Sci 2003, 88, 3132.
7. Khayet, M.; Suk, D. E.; Narbaitz, R. M.; Santerre, J. P.; Matsuura, T. J Appl Polym Sci 2003, 89, 2902.
8. Rana, D.; Matsuura, T.; Narbaitz, R. M.; Feng, C. J Membr Sci 2005, 249, 103.
9. Poussard, L.; Burel, F.; Couvercelle, J. P.; Merhi, Y.; Tabrizian, M.; Bunel, C. Biomaterials 2004, 25, 3473.
10. Gupta, T.; Pradhan, N. C.; Adhikari, B. J Membr Sci 2003, 217, 43.
11. Yang, J. M.; Lin, H. T.; Lai, W. C. J Membr Sci 2002, 208, 105.
12. Yang, J. M.; Lin, H. T. J Membr Sci 2001, 187, 159.
13. Huang, S. L.; Ou, C. F.; Lai, J. Y. J Appl Polym Sci 1999, 74, 1334.
14. Lee, K. R.; Teng, M. Y.; Hsu, T. N.; Lai, J. Y. J Membr Sci 1999, 162, 173.
15. Tanford, C. The Hydrophobic Effect: Formation of Micelles and Biological Membranes, 2nd ed.; Wiley: New York, 1980; Chapter 6, p 57.
16. Matsuura, T. Synthetic Membranes and Membrane Separation Processes; CRC: Boca Raton, FL, 1994.
17. Sourirajan, S.; Matsuura, T. Reverse Osmosis/Ultrafiltration Process Principles; National Research Council Canada: Ottawa, ON, 1985; Chapter 7, p 681.
18. Mosqueda-Jimenez, D. B.; Narbaitz, R. M.; Matsuura, T. J Environ Eng 2004, 130, 90.
19. Michaels, A. S. Sep Sci Technol 1980, 15, 1305.
20. Singh, S.; Khulbe, K. C.; Matsuura, T.; Ramamurthy, P. J Membr Sci 1998, 142, 111.
21. Zeman, L. J.; Zydney, A. L. Microfiltration and Ultrafiltration: Principles and Applications; Marcel Dekker: New York, 1996.
22. Binning, G.; Quate, C. F.; Gerber, Ch. Phys Rev Lett 1986, 56, 930.
23. Hansma, P. K.; Elings, V. B.; Marti, O.; Bracker, C. E. Science 1988, 242, 209.
24. Drake, B.; Prater, C. B.; Weisenhorn, A. L.; Gould, S. A. C.; Albrecht, T. R.; Quate, C. F.; Cannell, D. S.; Hansma, H. G.; Hansma, P. K. Science 1989, 243, 1586.
25. Fritzsche, A. K.; Arevalo, A. R.; Connolly, A. F.; Moore, M. D.; Elings, V.; Wu, C. M. J Appl Polym Sci 1992, 45, 1945.
26. Fritzsche, A. K.; Arevalo, A. R.; Moore, M. D.; Weber, C. J.; Elings, V. B.; Kjoller, K.; Wu, C. M. J Appl Polym Sci 1992, 46, 167.
27. Bowen, W. R.; Hilal, N.; Lovitt, R. W.; Williams, P. M. J Membr Sci 1996, 110, 229.
28. Bowen, W. R.; Hilal, N.; Lovitt, R. W.; Williams, P. M. J Membr Sci 1996, 110, 233.
29. Khulbe, K. C.; Kruczek, B.; Chowdhury, G.; Gagné, S.; Matsuura, T. J Appl Polym Sci 1996, 59, 1151.
30. Khulbe, K. C.; Kruczek, B.; Chowdhury, G.; Gagné, S.; Matsuura, T.; Verma, S. P. J Membr Sci 1996, 111, 57.
31. Lehmani, A.; Durand-Vidal, S.; Turq, P. J Appl Polym Sci 1998, 68, 503.
32. Khulbe, K. C.; Matsuura, T. Polymer 2000, 41, 1917.
33. Khulbe, K. C.; Feng, C. Y.; Tan, J. M. A. In Polyphenylene Oxide and Modified Polyphenylene Oxide Membranes: Gas, Vapor, and Liquid Separation; Chowdhury, G.; Kruczek, B.; Matsuura, T., Eds.; Kluwer Academic: Boston, MA, 2001; Chapter 8, p 231.
34. Norberg, D.; Holmquist, S.; Hong, S. K.; Taylor, J. S. In American Water Works Association: Membrane Technology Conference Proceedings, Atlanta, GA, March 2–5, 2003.
35. Kesting, R. E. J Polym Sci Part C: Polym Lett 1989, 27, 187.
36. Lau, W. W. Y.; Guiver, M. D.; Matsuura, T. J Membr Sci 1991, 59, 219.
37. Wang, D.; Li, K.; Sourirajan, S.; Teo, W. K. J Appl Polym Sci 1993, 50, 1693.
38. Hwang, J. R.; Koo, S.-H.; Kim, J.-H.; Higuchi, A.; Tak, T.-M. J Appl Polym Sci 1996, 60, 1343.
39. Grulke, E. A. In Polymer Handbook, 4th ed.; Brandrup, J.; Immergut, E. H.; Grulke, E. A., Eds.; Wiley: New York, 1999; Chapter VII, p 690.
40. Bloch, D. R. In Polymer Handbook, 4th ed.; Brandrup, J., Immergut, E. H., Grulke, E. A., Eds.; Wiley: New York, 1999; Chapter III, p 60.
41. Stamatialis, D. F.; Dias, C. R.; de Pinho, M. N. J Membr Sci 1999, 160, 235.
42. Khulbe, K. C.; Matsuura, T. J Membr Sci 2000, 171, 273.
43. Zeng, Y.; Wang, Z.; Wan, L.; Shi, Y.; Chen, G.; Bai, C. J Appl Polym Sci 2003, 88, 1328.
44. Kruczek, B.; Matsuura, T. J Appl Polym Sci 2003, 88, 1100.
45. Kwak, S.-Y.; Jung, S. G.; Yoon, Y. S.; Ihm, D. W. J Polym Sci Part B: Polym Phys 1999, 37, 1429.
46. Bessières, A.; Meireles, M.; Coratger, R.; Beauvillain, J.; Sanchez, V. J Membr Sci 1996, 109, 271.
47. Taniguchi, M.; Belfort, G. Langmuir 2002, 18, 6465.
48. Elimelech, M.; Zhu, X.; Childress, A. E.; Hong, S. J Membr Sci 1997, 127, 101.
49. Vrijenhoek, E. M.; Hong, S.; Elimelech, M. J Membr Sci 2001, 188, 115.
50. Bowen, W. R.; Doneva, T. A.; Stoton, J. A. G. Colloids Surf B 2002, 27,103.
51. Mosqueda-Jimenez, D. B.; Narbaitz, R. M.; Matsuura, T. Sep Purif Technol 2004, 37, 51.
52. Mosqueda-Jimenez, D. B.; Narbaitz, R. M.; Matsuura, T.; Chowdhury, G.; Pleizier, G.; Santerre, J. P. J Membr Sci 2004, 231, 209.
53. Mosqueda-Jimenez, D. B.; Narbaitz, R. M.; Matsuura, T. J Environ Eng 2004, 130, 1450.